



Self-healing of bio-cementitious mortar incubated within neutral and acidic soil

Mohamed Esaker · Omar Hamza · Adam Souid · David Elliott

Received: 25 July 2020 / Accepted: 26 March 2021
© The Author(s) 2021

Abstract The efficiency of bio self-healing of pre-cracked mortar specimens incubated in sand was investigated. The investigation examined the effect of soil pH representing industrially recognised classes of exposure, ranging from no risk of chemical attack (neutral pH ≈ 7) to very high risk (pH ≈ 4.5). Simultaneously, the soil was subjected to fully and partially saturated cycles for 120 days to resemble groundwater-level fluctuation. *Bacillus subtilis* with nutrients were impregnated into perlite and utilised as a bacterial healing agent. The healing agent was added to half of the mortar specimens for comparison purposes. Mineral precipitations were observed in both control and bio-mortar specimens, and the healing products were examined by SEM–EDX scanning. The healing ratio was evaluated by comparing (1) the repair rate of the crack area and (2) by capillary water absorption and sorptivity index—before and after incubation. The results indicated that bacteria-

doped specimens (bio-mortar) exhibited the most efficient crack-healing in all incubation conditions i.e. different chemical exposure classes. In the pH neutral soil, the average healing ratios for the control and bio-mortar specimens were 38% and 82%, respectively. However, the healing ratio decreased by 43% for specimens incubated in acidic soil (pH ≈ 4) compared with specimens incubated in neutral soil (pH ≈ 7). The study implies that bio self-healing is generally beneficial for concrete embedded within soil; however, aggressive ground conditions can inhibit the healing process.

Keywords Self-healing · Bio-concrete · Ground exposure conditions · Soil pH

Abbreviations

A_f	Final area of an individual crack
A_i	Initial area of an individual crack
BMS	Bio-mortar specimens
CMS	Control mortar specimens
EDX	Energy dispersive X-ray
h	Hour
I	Coefficient of absorption
PSD	Particle size distribution
RH	Relative humidity
S	Coefficient of sorptivity
SEM	Scanning electron microscope
t	Time

M. Esaker · O. Hamza (✉)
College of Engineering and Technology, University of Derby, Derby DE22 3AW, UK
e-mail: o.hamza@derby.ac.uk

A. Souid
Marie Skłodowska-Curie Postdoctoral Research Fellow,
College of Engineering and Technology, University of Derby, Derby, UK

D. Elliott
College of Natural and Life Sciences, University of Derby, Derby, UK



1 Introduction

Concrete is the most globally used construction material, and this is expected to be the case for the foreseeable future [1]. Despite its attractive properties, concrete requires regular maintenance to seal any appearing cracks in a timely manner [2] because cracks can increase the permeability of concrete, causing accelerated corrosion of the steel reinforcement and hence shorter service life. To address this issue and reduce the substantial costs of maintenance work, an innovative bacteria-based self-healing concrete (bio-concrete) has been developed over the last two decades [3–5].

The typical approach for preparing bio-self-healing concrete is to incorporate a suitable bacterial strain within the concrete mix to present viable bacteria throughout the finished product [6–9]. Once a crack occurs in the concrete, the encapsulated bacteria will be exposed at the crack surface and activated by contact with moisture from the surrounding environment. This approach places constraints upon the concrete formulation because it is necessary for the bacteria to survive the preparation and persist for the life of the structure in a suspended state. For this reason, hardy spore-forming bacteria are chosen, and they are often additionally encased or formulated with additives such as alginate or perlite for further protection. To facilitate the re-activation of bacteria after a crack event, a nutrition source may also be included in the formulation [e.g. 10]. Following the metabolic conversion of nutrients by bacteria in the presence of moisture and after a series of chemical reaction [11], the crack is sealed by precipitated calcium carbonate (CaCO_2).

Regardless of the types of bacterial-based approach, the provision of a suitable incubation environment is essential for the activation of bacteria and thus for a successful self-healing application. In the existing research on bio self-healing concrete, pre-cracked specimens have been subjected to various incubation scenarios. These denote either the external surroundings to which concrete may be exposed or are conditions conducive to healing. The specimens that exhibited successful healing had been either completely submerged in water throughout incubation or undergone wet-dry cycles. For example, Wang et al. [12] assessed the efficiency of self-healing in cracked

specimens exposed to four weeks of wet-dry cycles. These were submerged in tap water for 1 h and left to sit in the air with 60% RH at 20 °C for 11 h, which was then reduced by 2 h per day thereafter. Conversely, Luo et al. [13] explored three incubation conditions: (1) immersion in water; (2) 90% RH; and (3) wet-dry cycles, all at 25 °C. Throughout the wet–dry cycle of incubation, specimens were submerged in water for 12 h and then left to sit in the air for 12 h. For the specimens incubated in water and dry–wet cycles, the cracks were observed to have healed. By contrast, no healed cracks were observed for specimens incubated in the dry condition. This is because carbonation requires a suitable medium in which the carbon dioxide can dissolve and thus ensure the concrete maintains the pH value at a higher level.

The water used for incubation is generally distilled or tap water, although volatile diluted chloride solution [14–18] and de-icing salts may also be part of the surrounding environment [19]. For instance, Palin et al. [20] conducted an experiment in a low-temperature marine environment to assess the effectiveness with which bacteria-based methods can heal cracks. They immersed their cementitious samples in artificial seawater at 8 °C for 56 days. The permeability of 0.4 and 0.6 mm wide cracks was reduced by 95% and 93%, respectively. It may be the case that water contained a substance that could enhance the activity of bacteria, such as a source of food. To investigate this, Xu and Yao [21] assessed the efficacy of self-healing for specimens immersed in a solution comprising a source of calcium, yeast extract, and bacterial spores. The results indicated that 0.1–0.4 mm wide cracks were entirely sealed by calcium carbonate. In all the above studies, bacterial based self-healing was primarily explored under submerged conditions.

Whilst previous studies [22, 23] provided laudable advances in the understanding of bio self-healing concrete; it had limited relevance to the construction industry because the cementitious samples have been cured and incubated in limited types of environments (mainly water, seawater or humid air). However, in practice, significant parts of concrete structures are in interaction with the ground where cementitious materials are more likely to develop cracks at an early stage due to e.g. soil pressure or other mechanical and environmental exposures during the design life of the concrete. Secondly, the conventionally adopted prolonged water curing may not be available for some site



conditions. Thirdly, concrete structures (interacting with ground) are subjected to different geo-environmental exposures [24] e.g. acidic or alkaline soils. For structures in direct contact with soils posing a high risk of a chemical attack, bio self-healing concrete could be utilised to seal cracks and reduce such risk. This is especially important for underground concrete structures [25] because cracks can sometimes be extremely difficult to detect as they are surrounded by soil, and their locations are inaccessible.

The latest studies conducted by the authors [26, 27] have indicated that bio self-healing can be activated within the specimens' cracks under the saturated regime of cohesive soil (clay) as far as the matric suction (associated with the capillary effects) is smaller than the capillary pressure of the cracks. Expanding on this research, the present study reports further experimental work examining the bio self-healing concrete within non-cohesive soil (sand). The soil was subjected to fully and partially saturated cycles and conditioned with different pH and sulphate levels representing industrially recognised classes of exposure (namely, X0, XA1, and XA3). These classes were selected according to BS EN 206:2013 + A1:2016 [28]—based on the risk of corrosion and chemical attack from an aggressive ground environment, where X0 represents no risk and XA3 a very high risk. Cement mortar specimens (with and without bacterial agents) were utilised for the experiments, and their healing performance was evaluated by comparing the area repair rate and capillarity water absorption before and after the incubation within the soil. Optimal conditions for the practical application of bio self-healing within the soil were then discussed, which are highly relevant to structural and ground engineering as well as material science.

2 Materials and methods

2.1 Cultivation of bacterial strain

Bacillus subtilis (supplied by Philip Harris, UK) was utilised for the experimental programme. It was selected based on previous literature [29, 30] using similar strains and was driven largely by the ability of this genus to form resistant, long-lived spores. The bacterial strains were cultivated in Basal medium 121

and its derivatives 121A and 121B, as described by Sonenshein et al. [31]. The culture was incubated in a shaker at 125 rpm at a temperature of 36 °C for 72 h until the formation of spores was observed. This was confirmed under a microscope (LABOPHOT-2, Nikon) using the spore stain method. To minimise the presence of vegetative cells, spores were harvested using a centrifuge machine, where the culture was spun at high speed (3390 RCF) for 10 min and then washed twice using distilled water. Vegetative cells have been reported [32] to have an average density of 1.135 g/cm³, whereas the average spore density is 1.305 g/cm³. Therefore, the centrifugal force causes heavier particles to move away from the axis of rotation, resulting in the deposition of spores (forming what is known as a pellet) at the bottom of the test tube.

2.2 Encapsulation of spores into perlite

The main point of using capsules is to protect the healing agents (bacterial spores) from the harsh environment of fresh concrete such as high pH and temperature and also to prevent the agent from undesirable release during the mix. There are many approaches for encapsulation reported in the literature [33–35]. In this study, perlite was used to encapsulate the bacteria (with nutrients) due to its highly porous structure, which creates a suitable host environment for the healing agent. The properties of the used perlite were tested in accordance with British Standards [36, 37]; it had a unit weight of 128 kg/m³, porosity of 65% and moisture content of 22%. The particle size distribution of the perlite is illustrated in Fig. 1, which can be considered well-graded.

The perlite was first sterilised in the oven at a temperature of 160 °C for two days to destroy any microbes or bacteria present and remove moisture. To impregnate the perlite with bacterial spores, it was soaked in the bacterial suspension for 2 h until the suspension was absorbed. The surface of the perlite was then sprayed with a nutrient solution containing calcium acetate (60 g l⁻¹) and yeast extract (6 g l⁻¹). After each treatment, the perlite was dried in the oven at 40 °C for two days until a constant weight was obtained. These produced capsules containing approximately 0.3% of nutrients by perlite weight. The percentage of the nutrients was calculated by taking

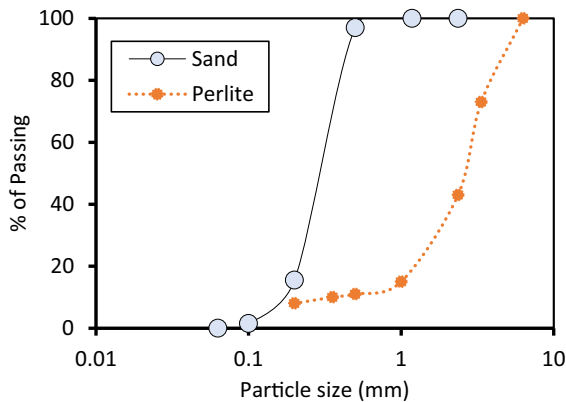


Fig. 1 Particle size distribution (PSD) of the Perlite and soil (sand)

the weight of the perlite before and after the impregnation.

The viability of bacterial spores in the perlite capsules was measured in terms of Colony Forming Unit (CFU). This was conducted according to the procedures described in Microbiology: laboratory manual [38]. Accordingly, the spore concentration contained in perlite capsules was approximately 6.4×10^7 CFU g^{-1} .

2.3 Preparation of specimens and crack creation

Control Mortar Specimens (CMS) and Bio-Mortar Specimens (BMS) were prepared according to BS EN 196-1. This was achieved by mixing Hanson Sulphate Resisting Cement (CEM III/A + SR), sand, tap water, and self-healing agent impregnated into perlite. The proportions of the mixture are given in Table 1. The water to cement ratio for all mixes was 0.5.

Two specimen geometries were prepared: (1) cylindrical specimens (with a diameter of 100 mm and a height of 40 mm) were used for the visual

inspection of crack sealing, and (2) prismatic specimens ($40 \times 40 \times 160$ mm) were used for water absorption testing. To avoid complete failure during crack propagation, the prisms specimens were reinforced by a fibre mesh placed at the centre of the specimens during casting. After 24 h, the mortar specimens were removed from their moulds and kept in water for a curing period of 28 days until they were tested.

After curing, the specimens were removed from the water and dried at room temperature in preparation for crack generation using standard mechanical testing. A three-point-bending test was used for the prisms and a splitting test for the cylinders. The prism was installed on two parallel beams at the bottom side, with the distance between them measuring approximately two-thirds of the total length of the sample. The top surface of the sample was compressed by one central beam. The induced cracks were controlled via Linear Variable Differential Transducers (LVDT) attached to the bottom of the specimens. The load was then applied gradually at a velocity of 0.001 mm s^{-1} until a crack was formed. The velocity was then decreased carefully to allow the crack to be formed around the specimen without failing it. The final load level was found to be in the range of 1.6–1.8 kN. The specimen was then unloaded, resulting in a decrease in crack width.

For the splitting test, the cylindrical specimens were wrapped with carbon fibre adhesive tape to prevent collapse during the formation of cracks under indirect tensile stresses. After placing the specimen horizontally between the upper and bottom plates in the uniaxial compressive strength test machine, the load was applied at low speed until a crack was observed on both sides of the cylinder. At this point, the loading was immediately stopped, and the specimen was removed for visual inspection under a light microscope (Nikon) where the widths of cracks were

Table 1 Mix proportion of the mortar specimens

Ingredient (Kg/m ³)	Mixture ID	
	Control mortar specimen (CMS)	Bio-mortar specimen(BMS)
Cement	450	450
Sand	761	761
Water	225	225
Perlite + bacteria + nutrients	–	22.5
Perlite	22.5	–

measured at regular intervals of 1 cm using Shuttlepix Editor software.

The inspection indicated that various cracks were generated with widths ranging between 60 and 350 μm as a result of the mechanical loading. Measuring and classifying these cracks were necessary to ensure each incubation environment would have similar ranges of crack widths.

2.4 Characterisation of soil and incubation process

The soil used in this study was sand with high-quality premium and free chemical with a sub-rounded grain shape. Typical sand was used for the incubation of bio and control mortar specimens. To characterise this soil, Particle Size Distribution (PSD) analysis was conducted using a sieve test in accordance with BS EN 933 [39]. The test confirmed that the soil was medium to fine sand BS 5930 [40], with 95–97% of the material between 100 and 700 μm and only around 3–5% smaller than 63 μm (Fig. 1). This sand is considered a permeable material with quick water drainage. Therefore, any induced change in water content or saturation degree (e.g. fully and partially saturated cycles required during the test) is expected to take effect quickly. In contrast to clay soils, such a change in water content could take an inordinately long time due to low permeability [41].

The chemical composition of the sand was also investigated under SEM and EDX. The results indicated that the sand was mainly composed of (SiO_2) Silicon dioxide, (K_2O) potassium oxide, (Al_2O_3) aluminium oxide, (Fe_2O_3) iron oxide, and (MgO) Magnesium oxide. This was similar to the SEM and EDX results conducted on the sand used for preparing the mortar mixture.

The sand was poured dry into plastic boxes (with dimensions of 35 \times 60 \times 40 cm) using a flexible hose attached to a sand hopper. The sand density (of $20.4 \pm 0.5 \text{ kN/m}^3$) was controlled by maintaining a constant drop height and flow rate. The sand was poured and levelled into two layers, the first one was below the specimens and another layer on top and between the specimens.

Up to 6 specimens were placed within each plastic box, which was previously outfitted with a filtration system containing a porous sheet and thin gravel layer, with an outlet at the base of these boxes for controlled

drainage. This setup (see Fig. 2) facilitated the creation of fully and partially saturated cycles during the incubation stage of the cracked specimens.

The pH value of the soil was adjusted to match the aggressive chemical environments with three categories X0, XA1, and XA3 classified in accordance with BS EN 206:2013 + A1:2016 [28]. X0 was the control class with a neutral pH value of around 7; whereas the pH values for classes XA1 and XA3 were adjusted to be approximately 6 (moderately acidic environment) and 4.5 (extremely acidic), respectively. As stated in BS 1377-3:1990 [42], Calcium sulphate is considered the sulphate salt that is most commonly found in soil. Therefore, the soil pH was reduced to the required level by mixing the soil with calcium sulphate (supplied by Sigma-Aldrich Ltd, UK) in the percentages shown in Table 2. For further confirmation, the soil pH was measured using a portable pH meter.

The cracked specimens were first visually inspected and tested for water absorption and then incubated at a depth of 20 cm from the bottom surface. The BMS and CMS specimens were incubated in separate boxes to avoid cross-contamination, i.e. immigrating the spores and nutrients from the crack zone of BMS specimens to CMS through water seepage within the soil. All incubations were conducted at a room temperature of approximately 23 $^\circ\text{C}$.

The cracked specimens were then incubated either in water or conditioned soil. The water incubation was used as a controlled environment where specimens were fully immersed during the entire incubation period. However, the conditioned soil was subjected to fully and partially saturated cycles for 120 days, as shown in Fig. 3. At the beginning of each cycle, the soil was made fully saturated by raising the water level above the mortar specimens up to the soil surface. Any loss of water (due to the natural evaporation) was compensated by regularly adding some water from the soil surface. This fully saturated stage lasted for 20 days, following which the test moved to the second stage (partially saturated stage) by allowing water to drain away from the soil at the bottom of the incubation box (Fig. 2). Because of the high permeability of sand, water drained away relatively fast (within 12 h) leaving the soil in a moist condition where the voids space became partially occupied by water. Based on the balance between the added and drained water, the degree of saturation was estimated at approximately $50 \pm 8\%$. This period of partially

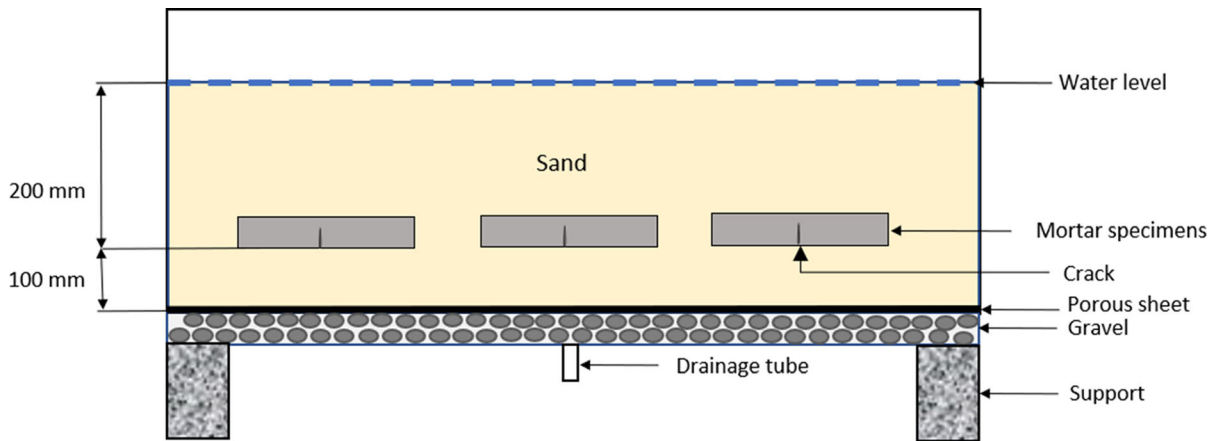


Fig. 2 Schematic illustration of an incubation box containing three cracked specimens in the sand

Table 2 Limiting values of calcium sulphate to achieve the desired exposure classes

Exposure class	X0	XA1	XA3
Calcium sulphate (mg/Kg)	0	≥ 2000 and ≤ 3000	$> 12,000$ and $\leq 24,000$
pH range	< 7.4 and ≥ 7	≤ 6.5 and ≥ 5.5	< 4.5 and ≥ 4
Achieved pH	7.2 ± 0.2	5.9 ± 0.2	4.3 ± 0.2

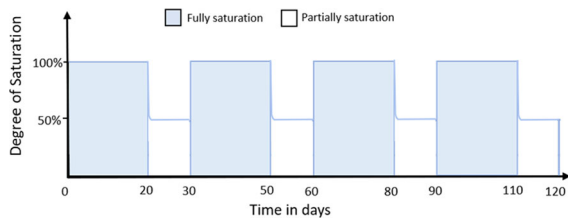


Fig. 3 Schematic illustration for fully and partially saturated cycles of incubation for a total period of 120 days

saturated condition was stopped after 10 days, and the soil was subjected to another fully and partially saturated cycles until the end of the incubation period (120 days).

During these cycles, the moisture content and pH level of the soil were regularly checked to ensure these were within the required range (Table 2). When the soil was partially saturated, we noticed some drop in pH level and moisture content, therefore it was necessary to recondition the soil by spraying its surface with some of the water previously drained from the soil (mixed with calcium sulphate if necessary).

3 Evaluation of crack healing efficiency

3.1 Visual inspection and image analysis

To evaluate the healing ratio, the cracked specimens were visually inspected before and after incubation using a digital microscope (Nikon P-400R, Japan). Immediately following their generation, each crack was marked at 3–4 positions distributed uniformly along its length. Photos of the marked cracks were taken before and after the incubation period. In preparation for the crack inspection, it was essential to conduct ultrasonic cleaning (within the water) after the soil incubation to remove any remaining soil particles. For each image, the crack width at each position near the markers was measured using ShuttlePix Editor Software (Nikon, Japan). Using a commercially available image processing programme called ImageJ [43], further analysis of the photos was then conducted to determine the healing ratio for all specimens. This software enables users to measure distances, areas, create density histograms, and other image analyses.

The healing ratio was measured as the decrease in the area fraction of each crack identified by black pixels corresponding to the cracks in a microscopic image after incubation (Fig. 4). A total of 72 microscopic images were taken along the lengths of the cracks and analysed using ImageJ software. The average healing ratio was calculated using Eq. 1.

$$\text{Average Healing Ratio} = \frac{1}{n} \sum_{i=1}^n (A_i - A_f) / A_i \quad (1)$$

where A_i and A_f are the initial and final area (respectively) of an individual crack at a certain location; and n = the total number of locations of the cracks analysed.

3.2 Capillary water absorption test

Concrete healing efficiency can also be evaluated by properties such as water absorption and chloride diffusion. Each of these can be measured using standardised procedures. Capillary water absorption is a non-destructive test linked to crack tightness and can, therefore, be used to quantify the water tightness of the specimens before and after cracking. According to Martys and Ferraris [44], the capillary suction is the result of unequal surface tension forces between the fluid–fluid and fluid–solid interfaces. Accordingly, the

water absorption rate in the capillary suction of the oven-dried mortar specimens was measured to calculate the sorption coefficient before and after the healing process.

The cracked prisms were oven-dried at a temperature of 40 °C for a minimum of one week until the mass-change in 2 h was less than 0.2% [45]. Before starting the test procedures, all mortar prisms sides were coated with epoxy resin to make them waterproof. The bottom surface was also coated with epoxy resin except for a small area of 20 mm × 40 mm around the crack. The initial weight of all specimens was recorded, and the test face of each specimen was placed on two plastic strips in a tray fitted with a loose lid to prevent air from moving around the specimens. The tray was filled with distilled water to a depth of approximately 2 mm above the level of the plastic strips.

The change in water absorption rate of the control (CMS) and bio-mortar specimens (BMS) before and after incubation was measured using an electronic balance with 0.01 g accuracy. To remove surface water, the specimens were wiped with a dampened cloth before taking their weights. The water uptake was measured frequently for 6 h (after 12 min, 30 min, 1 h, 2 h, 3 h, 4 h, and 6 h). The absorption and sorptivity coefficient (I and S) were calculated

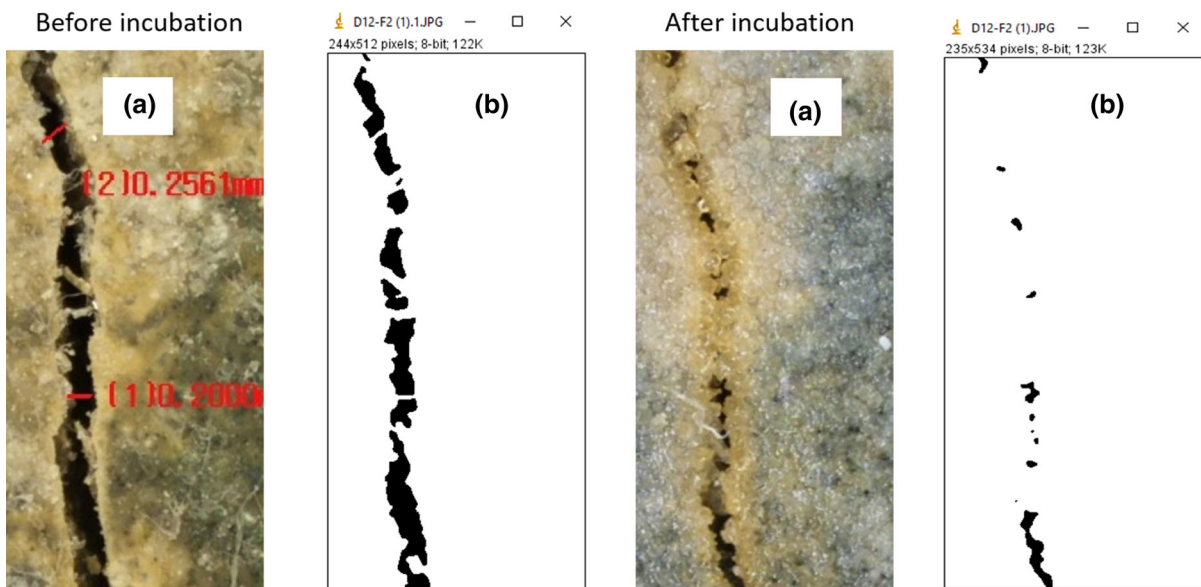


Fig. 4 Analysis of cracks' images before and after incubation using ImageJ software. **a** Cracks under ShuttlePix digital microscope, **b** binary images of crack

following BS EN 13,057:2002 [45]—based on the following equations.

$$I = \frac{m_t}{a \times d} \quad (2)$$

$$S = \frac{I}{\sqrt{t}} \quad (3)$$

where I = coefficient of absorption, m_t = change in specimen mass in grams at time t , a = exposed area of the specimen in mm^2 , d = density of the water in $\text{g}\cdot\text{mm}^{-3}$, S = coefficient of Sorption ($\text{mm}/\sqrt{\text{s}}$).

3.3 Characterisation of healing production

The crystalline structure and chemical compositions of the self-healing products for the control and bio-mortar specimens were characterised using a Scanning Electron Microscope (SEM) coupled with energy-dispersive X-ray spectroscopy (EDX). Following the visual inspection and water absorption test, the specimens were left for 48 h at room temperature until they were completely dry. They were then cut into small pieces around the healed crack to fit the chamber of the SEM machine and reduce the porous effect during the coating. The specimens were placed in a cylindrical disc chamber containing several holes in which to fix the sample for 10 min. This allowed a conductive layer of gold to form on the specimen surface, deposited by a low vacuum coating of the sample. An electron beam at a point on the top surface of the sample was then released in a raster pattern across the sample's surface to allow an image to form pixel by pixel.

4 Results and discussion

4.1 Visual evaluation of crack and healing quantification

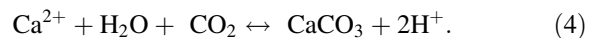
After 120 days of incubation, the control (CMS) and bio-mortar specimens (BMS) were removed from their incubation environments and visually inspected under the microscope to evaluate the crack closure. Figure 5 depicts several top views of the crack surface of BMS before and after the healing process in four different exposure conditions. As shown, the widths of completely healed cracks were significantly larger in

specimens incubated in water and pH neutral soil (X0) (280 and 260 μm , respectively) than specimens incubated in XA1 and XA3 (180 and 110 μm , respectively). In addition, only a few locations were completely healed for specimens incubated in XA3, which can be attributed to the effects of a high concentration of calcium sulphate and low soil pH.

The results of the microscopic inspection of CMS are presented in Fig. 6. This shows that most of the small cracks ($< 100 \mu\text{m}$) incubated under different conditions were autogenously healed (as a result of exposing the un-hydrated cement particles within the crack area to secondary hydration) and the maximum healed crack width was approximately 120 μm .

To quantify the healing ratio, images of cracks before and after incubation were analysed using ImageJ software. Table 3 presents the statistical results for the crack healing ratio of CMS and BMS specimens incubated in different exposure classes. The results of the image analysis were consistent with the microscopic observation. Furthermore, the relationship between the crack width and healing ratio for CMS and BMS was inverse in that the smaller the crack width, the higher the healing percentage.

As presented in Table 3, the healing percentage of CMS immersed in water was relatively high (42%) compared to the healing percentage of CMS in the soil of the exposure classes (38%, 37%, and 33% for X0, XA1, and XA3 respectively). The general process of bio self-healing is the precipitation of carbonate due to the equilibrium between Ca^{2+} and CO_2 with CaCO_3 (Eq. 4) [46], which is sensitive to pH (increased pH favours the production of carbonate).



In this process, CO_2 is produced by the activity of microorganisms and Ca^{2+} comes from the surrounding soil, water, and cement matrix, but can also be complexed with the microbial cell surface. Therefore, the lower healing efficiency observed in the exposure classes (Table 3) could be directly caused by the lower pH of these soils compared to the water. However, there is also likely to be a biological element and other abiotic factors influencing these results which is more difficult to resolve without further studies. For instance, the presence of soil matrix impedes the transportation of oxygen and other resources to the

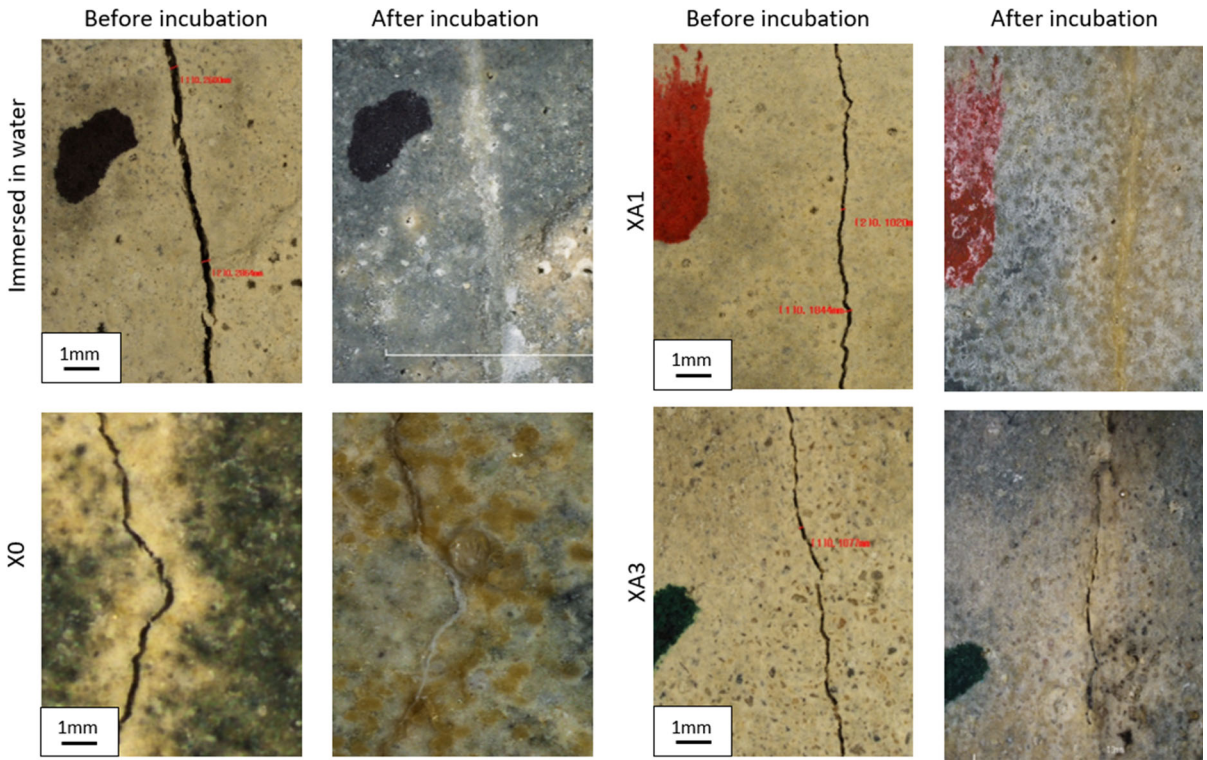


Fig. 5 Microscopic observation of crack healing of the bio mortar specimens (BMS) before and after 120 days of incubation

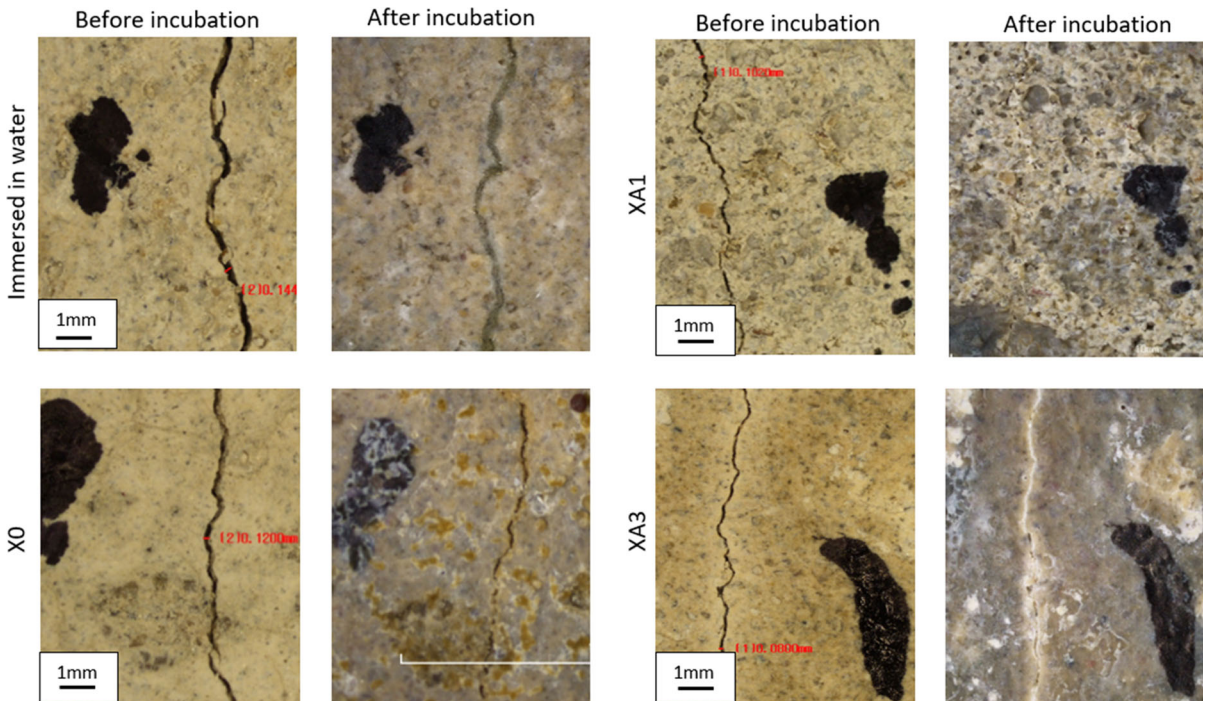


Fig. 6 Microscopic observation of crack healing of the control mortar specimens (CMS) before and after 120 days of incubation

Table 3 Statistical results of the crack healing ratio of CMS and BMS incubated under different exposure classes

Healing ratio (%)	Exposure classes							
	Water immersed		X0		XA1		XA3	
	CMS	BMS	CMS	BMS	CMS	BMS	CMS	BMS
Min	1.075	17.96	0.249	17.08	6.85	19.80	0.66	3.38
Max	99.062	99.74	84.71	100	94.15	99.96	90.27	99.05
Average	42.63	90.15	38.11	82.65	37.66	64.78	33.4	47.2
St. deviation	29.10	19.01	29.08	22.46	26.39	19.10	26.66	22.67

microbes, which could limit their capacity for CO₂ production.

Larger healing ratios were observed for all BMS compared to CMS; this accounts for the white mineral precipitation of calcium carbonate caused by the metabolic conversion of nutrients by bacteria [47], as evidenced by the EDX analysis. As indicated in Table 3, the soil pH has an influence on the performance of bio self-healing as the healing percentage of BMS incubated in XA3 is significantly lower (47%) than in the specimens incubated in X0 (82%). The highest healing percentage was approximately 90% for specimens immersed in water. This can be attributed to the high concentration of oxygen dissolved in water and light exposure, which stimulates the photosynthesis pathway of calcium carbonate precipitation [48].

These results indicate that using bacteria with cement-mortar could effectively improve the healing performance of cracks incubated within the ground. Moreover, a more efficient healing capacity was exhibited with specimens incubated in water and X0 than in those incubated in XA1 and XA3. The reduction in healing performance of BMS incubated in XA1 and XA3 can likely be attributed to the lower pH value in the surrounding environment.

4.2 Water absorption

The effect of each environmental exposure condition on the water absorption rate for CMS and BMS was examined before and after incubation (Fig. 7). The rate of water absorption through cracks due to capillarity water suction before and after incubation was compared to determine the direct relation between crack closure and absorption rate. The relationship between the mass of absorbed water per unit inflow area and the square root of time is illustrated in the

plots depicted in Figs. 8 and 9. The results show that after incubation, the sorptivity value for both types of specimens (CMS and BMS) decreased as a result of crack healing. However, this reduction was more evident in BMS, i.e. specimens impregnated with the bacterial agent.

The results also indicated that BMS incubated in exposure class X0 exhibited a higher reduction in absorption rate than specimens incubated in XA1 and XA3. For instance, the sorptivity indexes of the specimens incubated in X0, XA1, and XA3 were 3.262×10^{-5} , 4.394×10^{-5} and 6.465×10^{-5} mm/ $\sqrt{\text{sec}}$, respectively. As evident in the microscopic images and SEM results (presented in Sects. 4.1 and 4.3, respectively), high deposition of calcium carbonate filled the cracks, pores, and continuous channels that passed through the water and therefore reduced the absorption rate.

The absorption rate was higher and generally similar for CMS in all the exposure classes (X0, XA1 and XA3). However, a slight increase in absorption rate was observed for all specimens incubated in XA3.

It is evident that the sorptivity index values of the BMS were lower than those of the CMS in all environmental exposure conditions. For instance, the change in sorptivity index values for the BMS and CMS after incubation in X0 was 7.378×10^{-5} mm/ $\sqrt{\text{sec}}$ and 4.379×10^{-5} mm/ $\sqrt{\text{sec}}$, respectively. This implies that using bacteria with the cement mortar led to a 41% reduction in the sorptivity index values.

For the specimens CMS and BMS immersed in water, a relatively larger reduction in the sorptivity index (8.914×10^{-6} and 7.242×10^{-5} mm/ $\sqrt{\text{s}}$, respectively) was observed. This reduction was also in agreement with the image analysis, where more crack closure was observed in these specimens. Hence, as the crack closure (healing percentage) increases, the



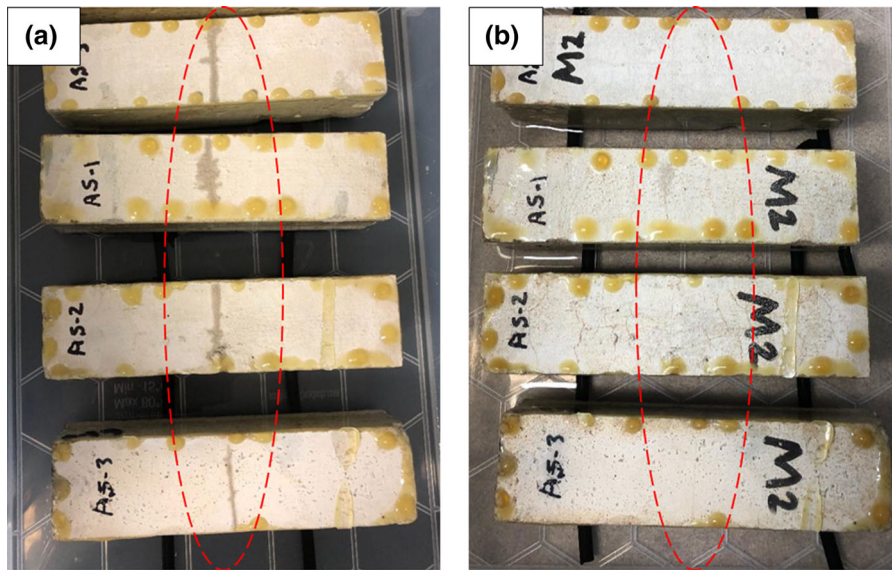


Fig. 7 Comparison of water absorbed by BMS after 2 h of absorption **a** Specimens before incubation, **b** the same specimens after incubation

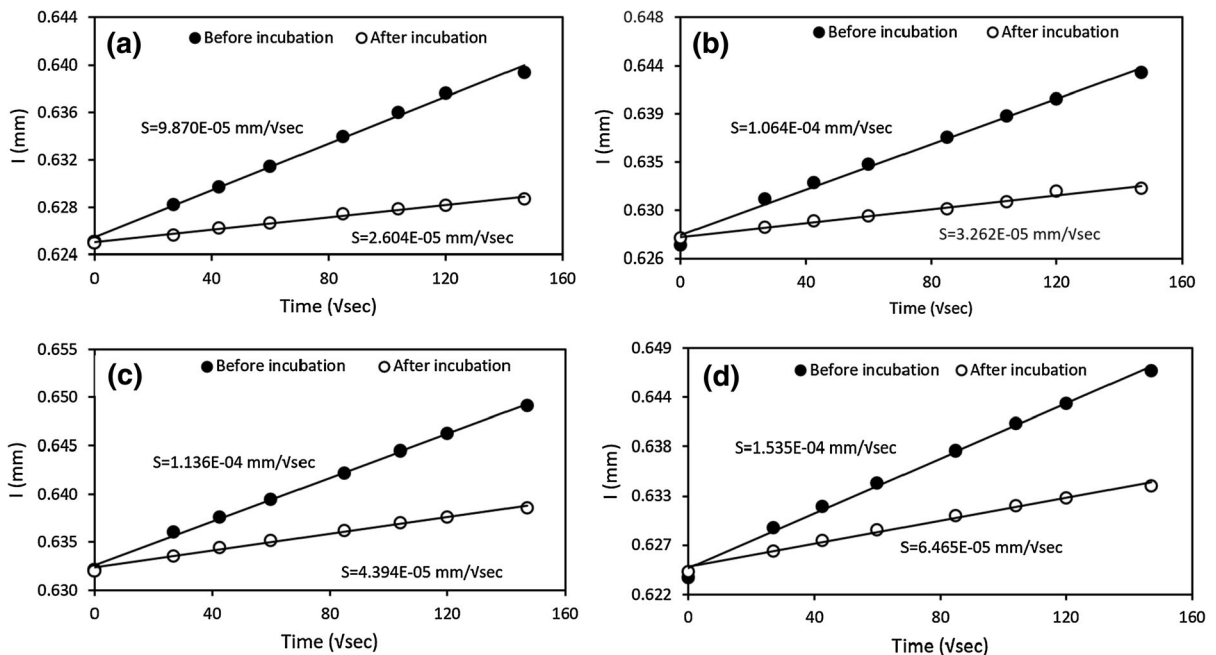


Fig. 8 Change in capillary water absorption of the BMS before and after 120 days of incubation in different environmental exposure conditions: **a** immersed in water, **b** X0-soil, **c** XA1-soil, and **d** XA3-soil

sorptivity index decreases because the closure alters the transport of moisture into the cracks of the tested specimens. These results (Fig. 10) indicate that healing ratios in water were generally larger than in sand, where pore-water in such porous media (sand) was less

available to support the bacterial activity. This implies that bio self-healing of concrete generally proceeds similarly within sand as has been previously reported for concrete incubated in humid air and water, where the best results have been achieved in water incubation

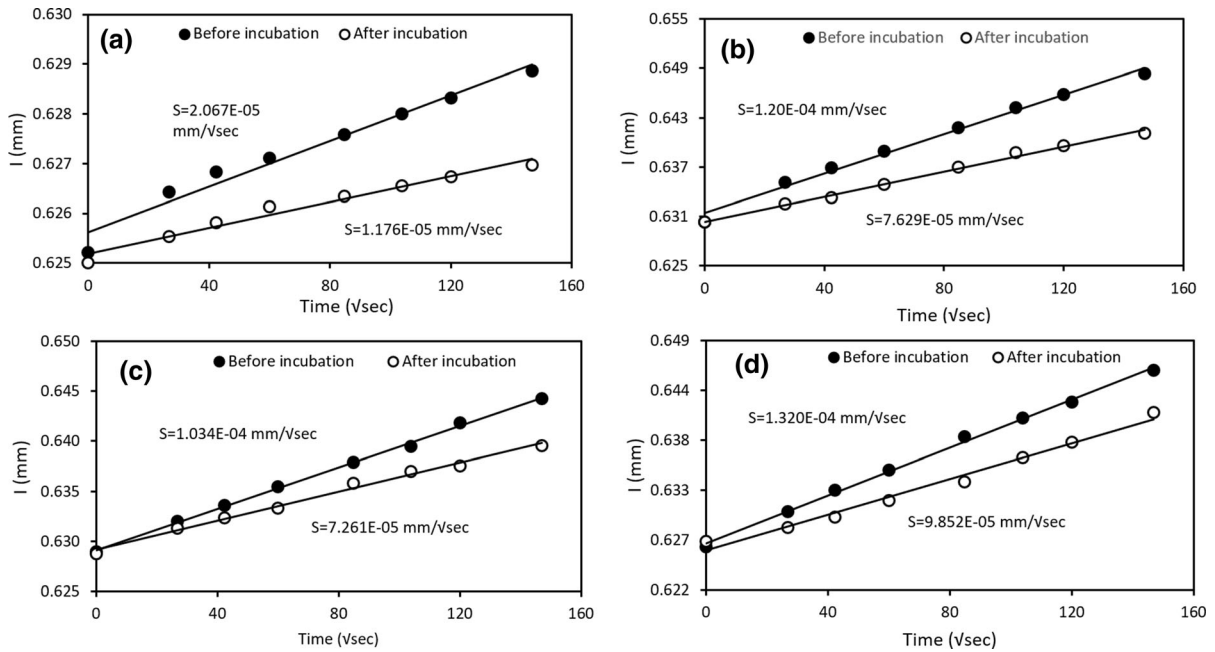


Fig. 9 Change in capillary water absorption of the CMS before and after 120 days of incubation (in different exposure conditions) **a** immersed in water, **b** X0-soil, **c** XA1-soil, and **d** XA3-soil

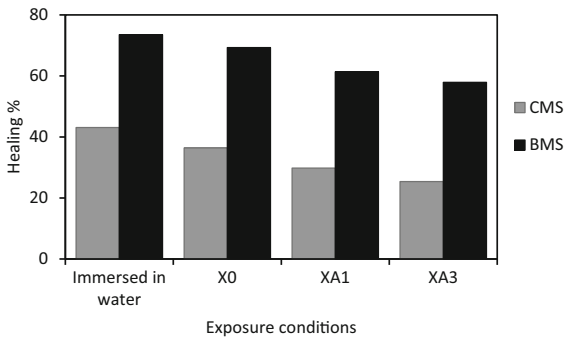


Fig. 10 The average healing percentages of BMS and CMS based on the change in water absorption rate before and after incubation under different exposure conditions

[13]. This might be attributed to several factors including the presence of moisture, dissolved oxygen, and partial pressure of carbon dioxide. For water incubation, cracked specimens were fully immersed in water for the whole incubation period, whereas, cracked specimens incubated in the sand were exposed to partially and fully-saturated cycles, therefore the repair effect underwater incubation was best and had a greater healing ratio in comparison with the sand.

4.3 Microstructure analysis of healing products

Figures 11 and 12 present the SEM results of CMS and BMS, respectively. The X-ray spectroscopy was conducted on a point, and the pixel size in SEM was between 6250 to 8435, whereas the acceleration voltage was 20KV.

The SEM analysis revealed that all specimens (BMS) incorporated with the bacterial agent contained regular and dense structure crystals of calcium carbonate. However, the density of the calcium carbonate crystals of the specimens incubated in XA3 was less than that of specimens incubated in X0 and XA1 (Fig. 12). This could be a result of the severe exposure condition and low pH (i.e. acidic environment).

The results of the EDX analysis of the healing products of BMS confirmed that the white precipitated materials on the crack surfaces were calcium carbonate, which is in line with the results obtained by other researchers [49, 50]. Therefore, it can be concluded that cracks were filled with calcium carbonate as a result of microbiologically induced calcite precipitation. By contrast, the microstructure analysis of CMS revealed that the main structure was formed by crystals of calcium hydroxide and ettringite (calcium

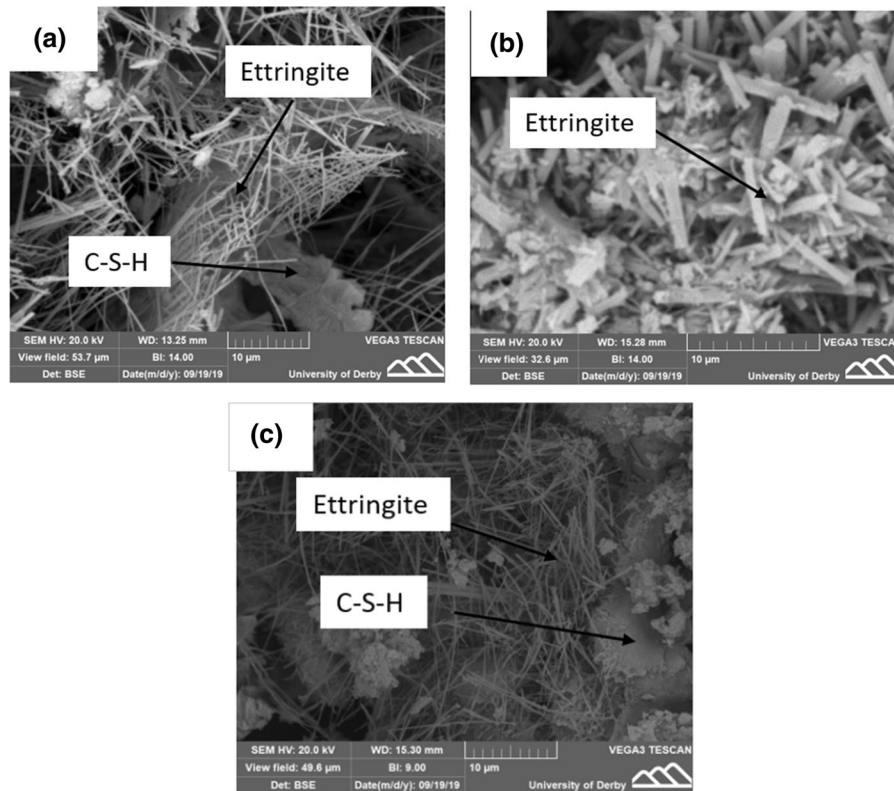


Fig. 11 a–c SEM images of healing products of control mortar specimens (CMS) incubated in X0, XA1, and XA3, respectively

sulphoaluminate) (Fig. 11). These were created as a result of the reaction of sulphate compounds with calcium aluminate in the cement and were similar to the crystals reported in a study conducted by Alghamri et al. [51]. The creation of ettringite crystals lowers the amount of calcium hydroxide (CH) and tricalcium aluminate (C_3A) in the cement-based matrix and the pressure of salt crystallisation inside the pores of the cement mortar [52, 53]. For all CMS, the EDX analysis of healing products in the cracks indicated the presence of Si and O. This can be attributed to the formation of calcium silicate hydrate (C–S–H) caused by the ongoing hydration of cement particles.

5 Conclusions

The study investigated the effect of different ground exposure conditions on the efficiency of bio self-healing concrete. Control and bio-mortar specimens (CMS and BMS) were incubated in sand with three pH values (7, 5.9, 4.5) representing three different classes

of exposure categorised following BS EN 206:2013 + A1:2016. Water curing was used as a controlled environment for both types of specimens. The feasibility and efficiency of self-healing were evaluated with reference to crack healing ratio and water tightness while the microstructure of the healing products was analysed and verified using SEM and EDX.

The results revealed that the healing ratio observed in specimens incubated in the sand was generally less than those incubated in water. This finding suggests that water incubation is still the most favourable environment for self-healing as maximum healing ratios were observed for both types of specimens (CMS and BMS).

The SEM and EDX results indicated that the mineral precipitations on the crack surfaces of the bio-mortar specimens (BMS) were calcium carbonate and that the healing products of control specimens (CMS) were ettringite and calcium silicate hydrate (C–S–H) caused by the ongoing hydration of cement particles.

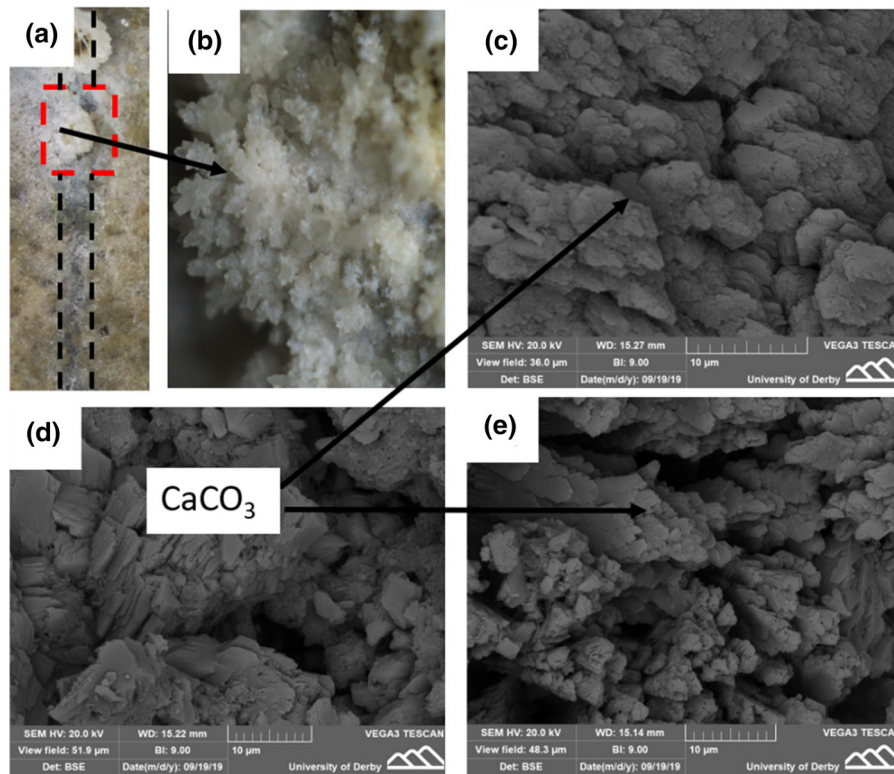


Fig. 12 SEM results of healing products of bio-mortar specimens (BMS): **a** microscopic image of crack-filled with white precipitation of calcium carbonate; **b** stereomicroscopic

close-up image (indicated by dotted square in image **(a)**) of calcium carbonate crystals; **c–e** SEM images of healing products of BMS incubated in X0, XA1, and XA3, respectively

Based on the statistical comparison of healing performance, the results showed efficient and notable self-healing for bio-mortar specimens (BMS) in comparison with control specimens (CMS) in all sand exposure conditions. For instance, using bacteria with cement mortar improved the crack healing ratio by more than 50% and reduced water absorption by more than 45% for specimens incubated in neutral sand (pH = 7).

However, the reduction in pH of the incubation environment affected bio self-healing performance. For instance, the healing percentage in the crack closure of specimens incubated in XA3 (pH = 4.5) was 43% lower than in specimens incubated in X0 (pH = 7). This indicates that for a cement-based material, bio self-healing is heavily reliant on external conditions.

The study also revealed that healing ratios in water were generally larger than in sand, where pore-water in such porous media was less available to support the bacterial activity. This implies that bio self-healing of

concrete generally proceeds in a similar fashion within sand as has been previously reported for concrete incubated in humid air and water, where the best results have been achieved in water incubation.

Notwithstanding these limitations, the study suggests that the bio self-healing process can protect underground concrete structures such as foundations, bridge piers, and tunnels in a range of standard exposure conditions and that this is facilitated by the commonly applied bacterial agent *B. subtilis*. However, as the experimental findings indicated that exposure conditions could affect the healing efficiency, future work should consider how formulations, application methods, and ground preparation can be optimised to achieve the best possible incubation environment and thus improved protection for underground concrete structures.

Acknowledgements The authors would like to thank Matt Whomsley, Ricard Duff and Graham Souch for their technical support during the experimental work.

Funding The study was funded by the University of Derby (Grant No. E&T-15- PGTA-0717). The study is also part of a project funded by the European Union's Horizon 2020 research and innovation programme under the Marie Skłodowska-Curie grant agreement No 798021.

Declarations

Conflict of interest The authors declare that they have no conflict of interest.

Open Access This article is licensed under a Creative Commons Attribution 4.0 International License, which permits use, sharing, adaptation, distribution and reproduction in any medium or format, as long as you give appropriate credit to the original author(s) and the source, provide a link to the Creative Commons licence, and indicate if changes were made. The images or other third party material in this article are included in the article's Creative Commons licence, unless indicated otherwise in a credit line to the material. If material is not included in the article's Creative Commons licence and your intended use is not permitted by statutory regulation or exceeds the permitted use, you will need to obtain permission directly from the copyright holder. To view a copy of this licence, visit <http://creativecommons.org/licenses/by/4.0/>.

References

- Zhang J, Liu Y, Feng T et al (2017) Immobilizing bacteria in expanded perlite for the crack self-healing in concrete. *Constr Build Mater* 148:610–617
- Chahal N, Siddique R, Rajor A (2012) Influence of bacteria on the compressive strength, water absorption and rapid chloride permeability of concrete incorporating silica fume. *Constr Build Mater* 37:645–651
- Wiktor V, Jonkers HM (2011) Quantification of crack-healing in novel bacteria-based self-healing concrete. *Cem Concr Compos* 33:763–770
- Kim H-K, Park S-J, Han J-I, Lee H-K (2013) Microbially mediated calcium carbonate precipitation on normal and lightweight concrete. *Constr Build Mater* 38:1073–1082
- Wang JY, De Belie N, Verstraete W (2012) Diatomaceous earth as a protective vehicle for bacteria applied for self-healing concrete. *J Ind Microbiol Biotechnol* 39:567–577
- Gupta S, Pang SD, Kua HW (2017) Autonomous healing in concrete by bio-based healing agents—a review. *Constr Build Mater* 146:419–428
- Xu H, Lian J, Gao M et al (2019) Self-healing concrete using rubber particles to immobilize bacterial spores. *Materials (Basel)*. <https://doi.org/10.3390/ma12142313>
- Jiang L, Jia G, Jiang C, Li Z (2020) Sugar-coated expanded perlite as a bacterial carrier for crack-healing concrete applications. *Constr Build Mater*. <https://doi.org/10.1016/j.conbuildmat.2019.117222>
- Singh H, Gupta R (2020) Cellulose fiber as bacteria-carrier in mortar: self-healing quantification using UPV. *J Build Eng*. <https://doi.org/10.1016/j.jobte.2019.101090>
- Wang J, Van Tittelboom K, De Belie N, Verstraete W (2012) Use of silica gel or polyurethane immobilized bacteria for self-healing concrete. *Constr Build Mater* 26:532–540
- Van Tittelboom K, De Belie N, De Muynck W, Verstraete W (2010) Use of bacteria to repair cracks in concrete. *Cem Concr Res* 40:157–166
- Wang JY, Snoeck D, Van Vlierberghe S et al (2014) Application of hydrogel encapsulated carbonate precipitating bacteria for approaching a realistic self-healing in concrete. *Constr Build Mater* 68:110–119
- Luo M, Qian C, Li R (2015) Factors affecting crack repairing capacity of bacteria-based self-healing concrete. *Constr Build Mater* 87:1–7
- Jonkers HM (2007) Self healing concrete: a biological approach. In: van der Zwaag S (eds) *Self healing materials*. Springer series in materials science, vol 100. Springer, Dordrecht. https://doi.org/10.1007/978-1-4020-6250-6_9
- Alder D, Lamont-Black J, Hamza O et al (2019) Validation of electrokinetic stabilisation of M5 Junction 7
- In CW, Holland RB, Kim JY et al (2013) Monitoring and evaluation of self-healing in concrete using diffuse ultrasound. *NDT E Int* 57:36–44. <https://doi.org/10.1016/j.ndteint.2013.03.005>
- Maes M, Snoeck D, De Belie N (2016) Chloride penetration in cracked mortar and the influence of autogenous crack healing. *Constr Build Mater* 115:114–124
- Maes M, Van Tittelboom K, De Belie N (2014) The efficiency of self-healing cementitious materials by means of encapsulated polyurethane in chloride containing environments. *Constr Build Mater* 71:528–537. <https://doi.org/10.1016/j.conbuildmat.2014.08.053>
- Cuenca E, Tejedor A, Ferrara L (2018) A methodology to assess crack-sealing effectiveness of crystalline admixtures under repeated cracking-healing cycles. *Constr Build Mater* 179:619–632. <https://doi.org/10.1016/j.conbuildmat.2018.05.261>
- Palin D, Wiktor V, Jonkers HM (2017) A bacteria-based self-healing cementitious composite for application in low-temperature marine environments. *Biomimetics* 2:13
- Xu J, Yao W (2014) Multiscale mechanical quantification of self-healing concrete incorporating non-ureolytic bacteria-based healing agent. *Cem Concr Res* 64:1–10
- Wu M, Hu X, Zhang Q et al (2019) Growth environment optimization for inducing bacterial mineralization and its application in concrete healing. *Constr Build Mater* 209:631–643. <https://doi.org/10.1016/j.conbuildmat.2019.03.181>
- Amer Algaifi H, Abu Bakar S, Mohd R, Sam A et al (2020) Insight into the role of microbial calcium carbonate and the factors involved in self-healing concrete. *Constr Build Mater* 254:119258. <https://doi.org/10.1016/j.conbuildmat.2020.119258>
- Hamza O, Bellis A (2008) Gault Clay embankment slopes on the A14—case studies of shallow and deep instability. In: Ellis NT, Yu H-S, Dawson A, McDowell G (eds) *Advances in transportation geotechnics*. CRC Press, London, pp 321–330
- Jin-long L, Hamza O, Sian Davies-Vollum K, Jie-qun L (2018) Repairing a shield tunnel damaged by secondary grouting. *Tunn Undergr Sp Technol* 80:313–321. <https://doi.org/10.1016/j.tust.2018.07.016>



26. Souid A, Esaker M, Elliott D, Hamza O (2019) Experimental data of bio self-healing concrete incubated in saturated natural soil. *Data Br* 26:104394. <https://doi.org/10.1016/j.dib.2019.104394>
27. Hamza O, Esaker M, Elliott D, Souid A (2020) The effect of soil incubation on bio self-healing of cementitious mortar. *Mater Today Commun* 24:100988. <https://doi.org/10.1016/j.mtcomm.2020.100988>
28. Institution BS BS EN 206:2013+A1:2016 Concrete. Specification, performance, production and conformity
29. Pei R, Liu J, Wang S, Yang M (2013) Use of bacterial cell walls to improve the mechanical performance of concrete. *Cem Concr Compos* 39:122–130. <https://doi.org/10.1016/j.cemconcomp.2013.03.024>
30. Kalhori H, Bagherpour R (2017) Application of carbonate precipitating bacteria for improving properties and repairing cracks of shotcrete. *Constr Build Mater* 148:249–260
31. Sonenshein AL, Cami B, Brevet J, Cote R (1974) Isolation and characterization of rifampin-resistant and streptolydigin-resistant mutants of *Bacillus subtilis* with altered sporulation properties. *J Bacteriol* 120:253–265
32. Tamir H, Gilvarg C (1966) Density gradient centrifugation for the separation of sporulating forms of bacteria. *J Biol Chem* 241:1085–1090. [https://doi.org/10.1016/s0021-9258\(18\)96806-7](https://doi.org/10.1016/s0021-9258(18)96806-7)
33. Alazhari M, Sharma T, Heath A et al (2018) Application of expanded perlite encapsulated bacteria and growth media for self-healing concrete. *Constr Build Mater* 160:610–619
34. Lee YS, Park W (2018) Current challenges and future directions for bacterial self-healing concrete. *Appl Microbiol Biotechnol* 102:3059–3070
35. De Belie N, Gruyaert E, Al-Tabbaa A et al (2018) A review of self-healing concrete for damage management of structures. *Adv Mater Interfaces* 5:1800074. <https://doi.org/10.1002/admi.201800074>
36. British Standards Institution, BS EN 1097-3:1998: Tests for mechanical and physical properties of aggregates. Determination of loose bulk density and voids
37. British Standards Institution, BS EN 1097-6:2013, Tests for mechanical and physical properties of aggregates. Determination of particle density and water absorption
38. Cappuccino J, Sherman N (2018) *Microbiology: a laboratory manual*, 11th edn. Pearson Education Limited, Harlow
39. British Standards Institution, BS EN 933-2:2020—Tests for geometrical properties of aggregates. Determination of particle size distribution. Test sieves, nominal size of apertures
40. British Standards Institution, BS 5930:1981—Code of practice for site investigations
41. Hamza O, Ikin J (2020) Electrokinetic treatment of desiccated expansive clay. *Géotechnique* 70:421–431. <https://doi.org/10.1680/jgeot.18.P.266>
42. Institution BS BS 1377-9: 1990 Methods of test for Soils for civil engineering purposes—Part 9: In-situ tests
43. Abramoff MD, Magalhaes PJ, Ram SJ (2004) Image Processing with Image. *J Biophoton Int* 11:36–42
44. Martys NS, Ferraris CF (1997) Capillary transport in mortars and concrete. *Cem Concr Res* 27:747–760. [https://doi.org/10.1016/S0008-8846\(97\)00052-5](https://doi.org/10.1016/S0008-8846(97)00052-5)
45. Institution BS BS EN 13057:2002, Products and systems for the protection and repair of concrete structures. Test methods. Determination of resistance of capillary absorption
46. Thomas AD, Dougill AJ, Elliott DR, Mairs H (2014) Seasonal differences in soil CO₂ efflux and carbon storage in Ntwetwe Pan, Makgadikgadi Basin, Botswana. *Geoderma* 219–220:72–81. <https://doi.org/10.1016/j.geoderma.2013.12.028>
47. Perito B, Mastromei G (2011) Molecular basis of bacterial calcium carbonate precipitation. *Prog Mol Subcell Biol* 52:113–139. https://doi.org/10.1007/978-3-642-21230-7_5
48. Seifan M, Samani AK, Berenjian A (2016) Bioconcrete: next generation of self-healing concrete. *Appl Microbiol Biotechnol* 100:2591–2602
49. Gupta S, Kua HW, Dai Pang S (2018) Healing cement mortar by immobilization of bacteria in biochar: an integrated approach of self-healing and carbon sequestration. *Cem Concr Compos* 86:238–254
50. Son H, Kim H, Park S, Lee H (2018) Ureolytic/non-ureolytic bacteria co-cultured self-healing agent for cementitious materials crack repair. *Materials (Basel)* 11:782. <https://doi.org/10.3390/ma11050782>
51. Alghamri R, Kanellopoulos A, Al-Tabbaa A (2016) Impregnation and encapsulation of lightweight aggregates for self-healing concrete. *Constr Build Mater* 124:910–921
52. Aye T, Oguchi CT (2011) Resistance of plain and blended cement mortars exposed to severe sulfate attacks. *Constr Build Mater* 25:2988–2996. <https://doi.org/10.1016/j.conbuildmat.2010.11.106>
53. Lee BY, Kurtis KE (2017) Effect of pore structure on salt crystallization damage of cement-based materials: Consideration of w/b and nanoparticle use. *Cem Concr Res* 98:61–70. <https://doi.org/10.1016/j.cemconres.2017.04.002>

Publisher's Note Springer Nature remains neutral with regard to jurisdictional claims in published maps and institutional affiliations.

